Tunable dark modes in one-dimensional "diatomic" dielectric gratings

Bo Zeng,[1] Arka Majumdar,[2] and Feng Wang[1,3,4,*]

[1]*Department of Physics, University of California at Berkeley, Berkeley, California 94720, USA*
[2]*Electrical Engineering, University of Washington, Seattle, Washington 98195, USA*
[3]*Material Science Division, Lawrence Berkeley National Laboratory, Berkeley, California 94720, USA*
[4]*Kavli Institute at University of California at Berkeley, Berkeley California, 94720, USA*
[*]*fengwang76@berkeley.edu*

Abstract: Recently researchers have demonstrated ultra high quality factor (Q) resonances in one-dimensional (1D) dielectric gratings. Here we theoretically investigate a new class of subwavelength 1D gratings, namely "diatomic" gratings with two nonequivalent subcells in one period, and utilize their intrinsic dark modes to achieve robust ultra high Q resonances. Such "diatomic" gratings provide extra design flexibility, and enable high Q resonators using thinner geometry with smaller filling factors compared to conventional designs like the high contrast gratings (HCGs). More importantly, we show that these high Q resonances can be efficiently tuned in situ, making the design appealing in various applications including optical sensing, filtering and displays.

References and links

1. M. El Beheiry, V. Liu, S. Fan, and O. Levi, "Sensitivity enhancement in photonic crystal slab biosensors," Opt. Express **18**(22), 22702–22714 (2010).
2. L. Shi, P. Pottier, Y.-A. Peter, and M. Skorobogatiy, "Guided-mode resonance photonic crystal slab sensors based on bead monolayer geometry," Opt. Express **16**(22), 17962–17971 (2008).
3. W. Suh, M. F. Yanik, O. Solgaard, and S. Fan, "Displacement-sensitive photonic crystal structures based on guided resonance in photonic crystal slabs," Appl. Phys. Lett. **82**(13), 1999 (2003).
4. R. Magnusson and S. S. Wang, "New principle for optical filters," Appl. Phys. Lett. **61**(9), 1022 (1992).
5. S. Peng and G. M. Morris, "Resonant scattering from two-dimensional gratings," J. Opt. Soc. Am. A **13**(5), 993 (1996).
6. S. Tibuleac and R. Magnusson, "Reflection and transmission guided-mode resonance filters," J. Opt. Soc. Am. A **14**(7), 1617 (1997).
7. S. S. Wang and R. Magnusson, "Theory and applications of guided-mode resonance filters," Appl. Opt. **32**(14), 2606–2613 (1993).
8. Q. Wang, D. Zhang, B. Xu, Y. Huang, C. Tao, C. Wang, B. Li, Z. Ni, and S. Zhuang, "Colored image produced with guided-mode resonance filter array," Opt. Lett. **36**(23), 4698–4700 (2011).
9. E.-H. Cho, H.-S. Kim, J.-S. Sohn, C.-Y. Moon, N.-C. Park, and Y.-P. Park, "Nanoimprinted photonic crystal color filters for solar-powered reflective displays," Opt. Express **18**(26), 27712–27722 (2010).
10. M. Boroditsky, T. F. Krauss, R. Coccioli, R. Vrijen, R. Bhat, and E. Yablonovitch, "Light extraction from optically pumped light-emitting diode by thin-slab photonic crystals," Appl. Phys. Lett. **75**(8), 1036 (1999).
11. A. Mekis, A. Dodabalapur, R. E. Slusher, and J. D. Joannopoulos, "Two-dimensional photonic crystal couplers for unidirectional light output," Opt. Lett. **25**(13), 942–944 (2000).
12. T.-C. Lu, S.-W. Chen, L.-F. Lin, T.-T. Kao, C.-C. Kao, P. Yu, H.-C. Kuo, S.-C. Wang, and S. Fan, "GaN-based two-dimensional surface-emitting photonic crystal lasers with AlN/GaN distributed Bragg reflector," Appl. Phys. Lett. **92**(1), 011129 (2008).
13. D. Fattal, J. Li, Z. Peng, M. Fiorentino, and R. G. Beausoleil, "Flat dielectric grating reflectors with focusing abilities," Nat. Photonics **4**(7), 466–470 (2010).
14. N. Yu and F. Capasso, "Flat optics with designer metasurfaces," Nat. Mater. **13**(2), 139–150 (2014).
15. J. D. Joannopoulos, P. R. Villeneuve, and S. Fan, "Photonic crystals: putting a new twist on light," Nature **386**(6621), 143–149 (1997).
16. P. C. Slabs, T. Asano, B. Song, Y. Akahane, and S. Noda, "Ultrahigh-Q nanocavities in two-dimensional photonic crystal slab," IEEE J. Sel. Top. Quantum Electron. **12**, 1123–1134 (2006).

17. D. K. Armani, T. J. Kippenberg, S. M. Spillane, and K. J. Vahala, "Ultra-high-Q toroid microcavity on a chip," Nature **421**(6926), 925–928 (2003).
18. J. Niehusmann, A. Vörckel, P. H. Bolivar, T. Wahlbrink, W. Henschel, and H. Kurz, "Ultrahigh-quality-factor silicon-on-insulator microring resonator," Opt. Lett. **29**(24), 2861–2863 (2004).
19. E. Chow, A. Grot, L. W. Mirkarimi, M. Sigalas, and G. Girolami, "Ultracompact biochemical sensor built with two-dimensional photonic crystal microcavity," Opt. Lett. **29**(10), 1093–1095 (2004).
20. S. Fan and J. Joannopoulos, "Analysis of guided resonances in photonic crystal slabs," Phys. Rev. B **65**(23), 235112 (2002).
21. Y. Yao, M. A. Kats, P. Genevet, N. Yu, Y. Song, J. Kong, and F. Capasso, "Broad electrical tuning of graphene-loaded plasmonic antennas," Nano Lett. **13**(3), 1257–1264 (2013).
22. S. S. Wang and R. Magnusson, "Design of waveguide-grating filters with symmetrical line shapes and low sidebands," Opt. Lett. **19**(12), 919–921 (1994).
23. V. Karagodsky and C. J. Chang-Hasnain, "Physics of near-wavelength high contrast gratings," Opt. Express **20**(10), 10888–10895 (2012).
24. S. S. Wang and R. Magnusson, "Multilayer waveguide-grating filters," Appl. Opt. **34**(14), 2414–2420 (1995).
25. A. Sharon, D. Rosenblatt, and A. A. Friesem, "Narrow spectral bandwidths with grating waveguide structures," Appl. Phys. Lett. **69**(27), 4154 (1996).
26. S. Zhang, D. A. Genov, Y. Wang, M. Liu, and X. Zhang, "Plasmon-induced transparency in metamaterials," Phys. Rev. Lett. **101**(4), 047401 (2008).
27. M. I. Stockman, S. V. Faleev, and D. J. Bergman, "Localization versus delocalization of surface plasmons in nanosystems: can one state have both characteristics?" Phys. Rev. Lett. **87**(16), 167401 (2001).
28. B. Luk'yanchuk, N. I. Zheludev, S. A. Maier, N. J. Halas, P. Nordlander, H. Giessen, and C. T. Chong, "The Fano resonance in plasmonic nanostructures and metamaterials," Nat. Mater. **9**(9), 707–715 (2010).
29. N. Verellen, Y. Sonnefraud, H. Sobhani, F. Hao, V. V. Moshchalkov, P. Van Dorpe, P. Nordlander, and S. A. Maier, "Fano resonances in individual coherent plasmonic nanocavities," Nano Lett. **9**(4), 1663–1667 (2009).
30. N. Liu, L. Langguth, T. Weiss, J. Kästel, M. Fleischhauer, T. Pfau, and H. Giessen, "Plasmonic analogue of electromagnetically induced transparency at the Drude damping limit," Nat. Mater. **8**(9), 758–762 (2009).
31. V. Karagodsky, F. G. Sedgwick, and C. J. Chang-Hasnain, "Theoretical analysis of subwavelength high contrast grating reflectors," Opt. Express **18**(16), 16973–16988 (2010).
32. A. Chandran, E. S. Barnard, J. S. White, and M. L. Brongersma, "Metal-dielectric-metal surface plasmon-polariton resonators," Phys. Rev. B **85**(8), 085416 (2012).
33. T. Ochiai and K. Sakoda, "Dispersion relation and optical transmittance of a hexagonal photonic crystal slab," Phys. Rev. B **63**(12), 125107 (2001).
34. F. Lemarchand, A. Sentenac, and H. Giovannini, "Increasing the angular tolerance of resonant grating filters with doubly periodic structures," Opt. Lett. **23**(15), 1149–1151 (1998).
35. A.-L. Fehrembach, A. Talneau, O. Boyko, F. Lemarchand, and A. Sentenac, "Experimental demonstration of a narrowband, angular tolerant, polarization independent, doubly periodic resonant grating filter," Opt. Lett. **32**(15), 2269–2271 (2007).
36. F. Lemarchand, A. Sentenac, E. Cambril, and H. Giovannini, "Study of the resonant behaviour of waveguide gratings: increasing the angular tolerance of guided-mode filters," J. Opt. A, Pure Appl. Opt. **1**(4), 545–551 (1999).
37. A. Mizutani, H. Kikuta, and K. Iwata, "Wave Localization of Doubly Periodic Guided-mode Resonant Grating Filters," Opt. Rev. **10**(1), 13–18 (2003).
38. R. Zengerle, "Light Propagation in Singly and Doubly Periodic Planar Waveguides," J. Mod. Opt. **34**(12), 1589–1617 (1987).
39. S. T. Peng, "Rigorous formulation of scattering and guidance by dielectric grating waveguides: general case of oblique incidence," J. Opt. Soc. Am. A **6**(12), 1869–1883 (1989).
40. S. T. Thurman and G. M. Morris, "Controlling the spectral response in guided-mode resonance filter design," Appl. Opt. **42**(16), 3225–3233 (2003).
41. M. G. Moharam, E. B. Grann, D. Pommet, and T. K. Gaylord, "Formulation for stable and efficient implementation of the rigorous coupled-wave analysis of binary gratings," J. Opt. Soc. Am. A **12**(5), 1068 (1995).
42. S. Fan, W. Suh, and J. D. Joannopoulos, "Temporal coupled-mode theory for the Fano resonance in optical resonators," J. Opt. Soc. Am. A **20**(3), 569–572 (2003).
43. N. Liu, M. Mesch, T. Weiss, M. Hentschel, and H. Giessen, "Infrared perfect absorber and its application as plasmonic sensor," Nano Lett. **10**(7), 2342–2348 (2010).
44. F. Wang and Y. R. Shen, "General properties of local plasmons in metal nanostructures," Phys. Rev. Lett. **97**(20), 206806 (2006).
45. R. Magnusson and M. Shokooh-Saremi, "Widely tunable guided-mode resonance nanoelectromechanical RGB pixels," Opt. Express **15**(17), 10903–10910 (2007).

1. Introduction

Planar optical resonators with high quality factor (Q) modes play crucial roles in modern photonic technologies, with applications ranging from sensing [1–3], filtering [4–7], display

[8–10] to laser and optical interconnects [11,12]. The planar design has attracted much attention in research because of its benefits of easy fabrication and potential compatibility for on-chip integration with other optoelectronic components [13–15]. Compared to the small mode-volume and defect-based counterparts [16–19], delocalized modes, most notably the guided waves in photonic crystal slabs, allow free space excitation and better coupling efficiency with quantum well or 2D materials like graphene or transition metal dichalcogenides [14,20,21]. Ultra high Q resonances in photonic crystal slabs have been proposed and demonstrated in various designs, a recent example being the high contrast gratings (HCG) [7,22,23]. However, their optimization towards thickness and tunability is generally lacking.

Here, we study a new class of subwavelength 1D dielectric gratings with two nonequivalent subcells in each period, referred to as "diatomic" gratings. These "diatomic" gratings have great design flexibility as they support structurally defined "dark modes". Q factors of these "dark modes" are robust against strong external perturbation and their resonance can be tuned continuously, for instance, by mechanically stretching the grating in situ. When suspended in air, our optimized "diatomic" design boasts a much thinner geometry, higher Q and better in situ tunability compared to conventional HCGs [24,25]. At resonance, electrical fields of the "diatomic" grating are largely concentrated in its air gap. The "diatomic" grating acts effectively as a thin layer of low refractive index medium with tunable resonances and exposed fields, making it potentially a useful platform to various applications including optical sensing, filtering and displays.

2. Theory

A "dark" mode is an electromagnetic eigenmode of an optical system that has very small radiative coupling (κ) to far fields [26,27]. The concept of "dark" mode is central to many novel optical phenomena including Fano resonance (FR) and electromagnetically induced transparency (EIT) [28–30]. For an optical cavity, κ is usually related to $1-|r|^2$, where r is the mode reflectivity at the cavity interfaces (e.g. $z=0$ or $z=t$ in Fig. 1(a)). Compared with "bright" modes, photons in a "dark" mode experience longer lifetime in the cavity and thus higher Q because of the effectively larger r. This leads to ultra high Q resonances in dielectric structures where other types of photonic energy loss is negligible.

For a guided mode in subwavelength gratings, κ is qualitatively determined by the field overlap between this mode and the zero-th order reflection or transmission plane wave at the interfaces $z=0,t$ respectively [31,32]. In particular, with normal incidence and TM polarization which is our main focus in this paper, κ can be written as:

$$1-|r|^2 \equiv \kappa \propto \frac{\left|\int_0^P E_x dx\right|^2_{z=0,t}}{P} \tag{1}$$

where P is the period of the grating and E_x is the x component of the electrical field of the mode at the interface $z=0$ or $z=t$. r and κ are the same for both reflection ($z=0$) and transmission ($z=t$) interfaces when the grating is suspended in air.

The reduced Brillouin zone and coupling behavior of a regular subwavelength 1D grating (schematic view in Fig. 1(a)) is illustrated in Fig. 1(b). With normal incidence, only modes at the zone center (Γ point) can be excited in the grating, if scattering from grating edges are to be ignored. Due to the overall reflection symmetry of the 1D grating, both even and odd modes are present at the zone center. The even modes are "bright" modes that couple strongly to the far-field radiation (red dots in Fig. 1(b)), and the odd modes are completely "dark" with zero coupling (dark dots) [33].The modes at finite k_x, in particular those close to the zone edge, cannot couple to the normal incident because of large momentum mismatch. Those

modes (gray dots) are otherwise considered "dark" because $\kappa \approx 0$ owing to the field's sign change in one unit cell ($k_x \rightarrow \pi / P$).

The "dark" modes at zone edge can be folded back to Γ point by breaking the symmetry of adjacent unit cells in the grating, after which they gain a small but finite κ to the normal incidence. In this process, which is also known as "zone folding", two adjacent unit cells (referred here as subcell 1 and subcell 2) merge into a bigger one, illustrated in Fig. 1(c). We call such 1D gratings with two subcells in one period "diatomic" gratings. It is worth noting that a similar symmetry breaking concept, called the "doubly periodic grating", has been previously proposed to improve the angular tolerance of guided mode resonances [34–38]. However, the Q of these resonators remain relatively low (~8,000) and their dark mode aspects are largely unexplored.

One can engineer the asymmetry between the subcells to control the behavior of the grating with great flexibility. Here we focus on the cases that the two subcells are identical except for their air gaps. This asymmetry is captured by $\delta = \dfrac{|a_1 - a_2|}{P}$, where a_1 and a_2 are the widths of the corresponding air gaps and P is the grating period. We also denote $\gamma = \dfrac{2s}{P}$ as the dielectric filling factor where s is the width for each dielectric bar in the subcells (Fig. 1(c)). In our case, the dielectric bar is made of silicon ($n_{dielectric} = 3.48$). When $\delta = 0$, the design is identical to a regular grating. However, when $\delta \neq 0$, the zone edge "dark" modes are folded back to Γ point in the Brillouin Zone with finite κ, shown as the gray dots in Fig. 1(d). It is important to note that the 1st order "dark" mode (the gray dot in the dashed blue curve of Fig. 1(d)) is guaranteed to exist in the subwavelength regime as long as $\gamma \neq 0$ and $n_{dielectric} > 1$, even at large incidence angles when $k_x \gg 0$. This is easily checked as the result of gap opening due to the non-uniform $\varepsilon(x)$ in the grating. The dispersion of the fundamental mode (blue curve) in Fig. 1(b) always bends downwards from the light cone, ensuring $\omega_{\text{1st dark mode}} < \dfrac{2\pi c}{P}$. The emergence of these "dark" modes in the zone center can also be viewed as mode splitting in Fig. 1(e), where a pair of even and odd modes are created from the originally "bright" mode after symmetry breaking. The odd mode has weak coupling to far field radiation due to the destructive interferences from its two subcells, corresponding to a "dark" mode. Typical electrical field profiles for the 1st order "bright" and "dark" modes of the "diatomic" grating ($\delta = 0.05, \gamma = 0.2$) are shown in Fig. 1(f). The mode profiles and band structures in the Brillouin zone are calculated using numerical methods described in [39].
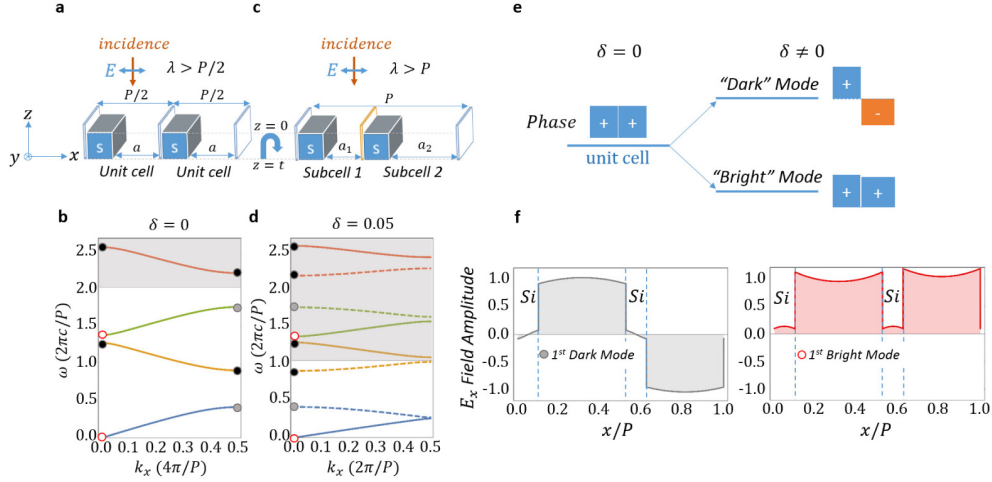
Fig. 1. Design of the "Diatomic" grating and the emergence of intrinsic "dark" modes. (a) Schematic diagram of a regular grating. Grating is excited with normal incidence and TM polarization. Thickness t, period $P/2$ and filling factor γ are given as grating parameters. Incidence and Transmission interfaces of the grating are at $z = 0$ and $z = t$, respectively. Blue blocks represent dielectric bars with width s. The one dimensional grating is assumed to be infinitely long in the y direction. (b) Brillouin zone of a typical regular grating with $\gamma = 0.2$. Red dots represent "bright" modes at the zone center and dark dots represent completely "dark" modes due to reflection symmetries in the grating. Gray dots represent "dark" modes with a small but finite κ at the zone edge. Shaded area indicates frequencies outside the subwavelength regime ($\omega > 4\pi c/P$ and $\omega > 2\pi c/P$ for the regular and "diatomic" gratings respectively). (c) Schematic diagram of a "diatomic" grating with the same filling factor $\gamma = 0.2$ except for a doubled period P and finite air gap difference δ. Two subcells merge into a larger unit cell. (d) Brillouin zone of a typical "diatomic" grating with $\delta = 0.05$. Note the Brillouin zone is folded with half the original size. (e) Illustration of emergence of a pair of "bright" and "dark" modes after symmetry breaking. The "dark" mode has field phases difference of nearly π in its 2 subcells. (f) The field profile for E_x for the 1st order "bright" and "dark" eigenmodes in the "diatomic" design.

The "diatomic" structure is completely defined with three parameters: grating period (P), dielectric filling factor (γ) and the subcell difference (δ). When $\delta \neq 0$ but $\delta \ll 1$ (that is, $|a_1 - a_2| \to 0$), it is straightforward to estimate the coupling coefficient κ for the "dark" modes represented in Fig. 1(e):

$$\kappa \propto \frac{\left| \int_0^P E_x dx \right|^2}{P} = \frac{\left| \int_0^{s+a_1} E_x dx - \int_{s+a_1}^P E_x dx \right|^2}{P} \propto \delta^2 \to 0 \tag{2}$$

Equation (2) follows because for small δ, the mode profile in subcell 1 and subcell 2 are approximately the same except for a sign change. The "diatomic" design not only makes those "dark" modes accessible to zone center excitation, but more importantly, it can engineer their "darkness" (κ) by proper choice of δ. In addition, Eq. (2) depends solely on the design (P, γ, δ) itself. As a result, the Q and the existence of these "dark" modes are expected to be robust even under strong external perturbation.

3. Design

Qualitatively speaking, grating resonances occur when the guided eigenmodes bounce back and forth constructively from the interfaces ($z = 0, t$), forming an F-P like cavity [40]. Above

the cut-off frequency, each eigenmode in the grating can display its own resonance whenever the round trip phase condition $\phi_{round} = 2\pi n$ is satisfied and the Q is determined by κ respectively. With the guaranteed existence discussed above, we expect to see ultra high Q resonance of the 1st order "dark" mode in the "diatomic" gratings.

Figure 2(b) shows the simulated reflection spectrum for various filling factors γ in a thin "diatomic" grating using rigorous coupled-wave analysis (RCWA) [41]. The grating design parameters are $\delta = 0.05$ and $t / P = 0.1$. Focusing on the sharp resonance of the "dark" mode, we see marked decline in Q (Fig. 2(a)) from 10^8 to 10^5 with γ varying from 0.1 to 0.5. The resonance wavelength λ_{res} is slightly red-shifted due to a larger n_{eff}. The fall in Q can be qualitatively understood by an increased mixing between "dark" and "bright" modes in the grating [31], leading to reduced effective $|r|$ for the "dark" mode. Intuitively, an increase in γ (thus n_{eff}) helps to excite more "bright" modes in the grating and as a result, photonic loss rises in general because of their contribution of stronger coupling to the far fields.
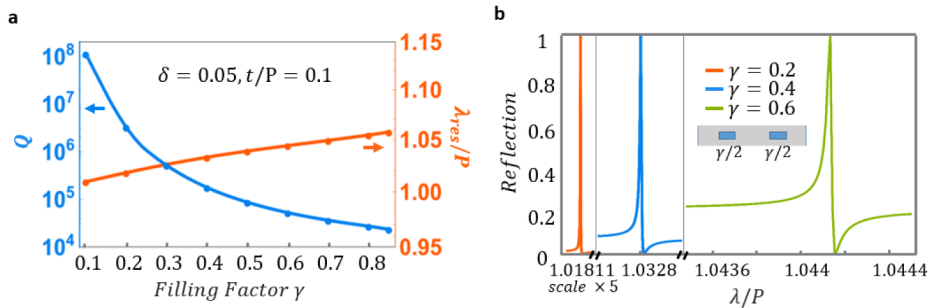

Fig. 2. Dependence of Q on filling factors for the "diatomic" design: the thin grating case. (a) Dramatic decline in Q for the dark mode resonance as a result of increased filling factor and subsequent increased mixing with "bright" modes. (b) Reflection spectrum showing resonances of varying Q for 3 different filling factors. Inset shows a unit cell of the "diatomic" grating with given design parameters assuming $P = 1$ and colored blocks represent silicon bars. The x axis is wavelength λ normalized by period P. For the leftmost spectrum with $\gamma = 0.2$, scale of x axis is magnified by 5 for clarity.

We study the Q dependence on γ more carefully with an example of a thicker "diatomic" grating. For design parameters $\delta = 0.05$ and $t / P = 0.5$, we see in Fig. 3(a) that indeed more "bright" mode resonances are present with larger γ, producing complex beating patterns as an unfavorable spectroscopic background. The presence of "bright" modes is more pronounced in a thick grating compared to thinner ones. In Fig. 3(a), each of the sharper resonances corresponds to a "dark" mode, while λ_{res} is determined with round trip condition $\phi_{round} = 2\pi n$ (color line in Fig. 3(c)). A closer look at Fig. 3(b) reveals that the reflectivity $|r|$ at the corresponding first order λ_{res} ($\phi_{round} = 2\pi$, color markers in Fig. 3(c)) falls as γ is increased. One can also verify that with larger γ, more "bright" modes (gray lines in Fig. 3(c) and Fig. 3(b)) with much smaller $|r|$ start to resonate. The exact behavior of mixing between "dark" and "bright" modes is complicated but it explains well the declining trend of quality factors seen in Fig. 3(a). We conclude that Q degrades with γ. Our observation also reflects the difficulty to achieve high Q resonances in a beat free background in other grating designs like the HCG, as they generally rely on a complicated mixing of "bright" modes that requires large grating thicknesses [23].
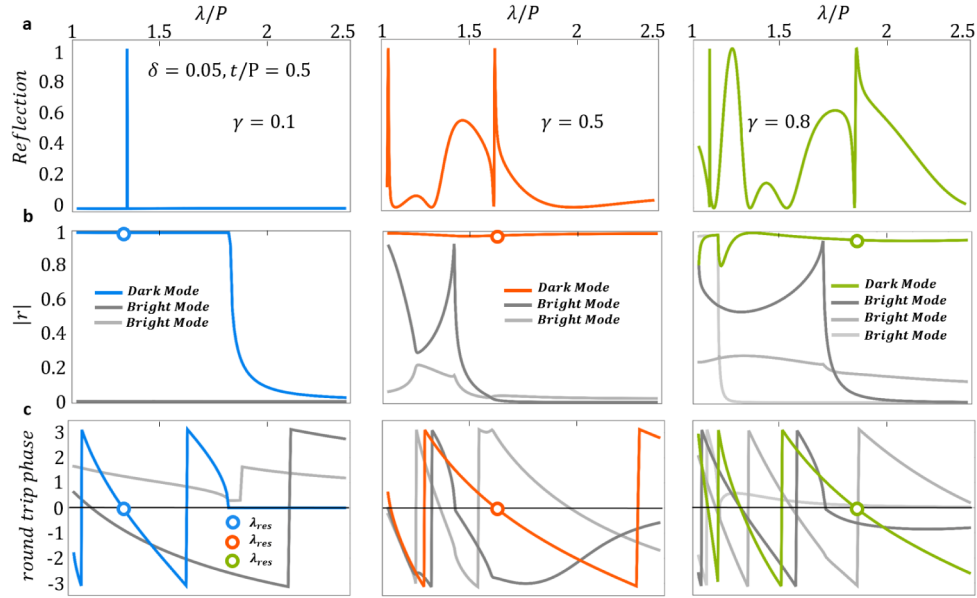
Fig. 3. Demonstration of the effect of filling factors on the "diatomic" design. (a) Emergence of beating patterns from additional "bright" mode resonances for large filing factor γ in a thicker grating design. x axis is wavelength (λ) normalized by grating period (P). (b) Effective $|r|$ for the "dark" mode (color line) and "bright" modes (gray lines) with different γ. The trend in $|r|$ for corresponds well with decline in Q for the "dark" mode. (c) Round trip phase for "bright" (gray) and "dark" modes (color). It predicts well where the first "dark" mode resonance is (color markers, when $\phi_{round} = 2\pi n, n = 1$) and shows the emergence of new resonances from "bright" modes as γ increases.

We can then optimize the "dark" mode performance by choosing a small γ and small grating thickness to minimize mode "mixing" in "diatomic" gratings. In Fig. 4(a), we show a characteristic single high Q ($\sim 10^6$) resonance under TM and normal incidence (red curve) for the "diatomic" grating. The design parameters are $\gamma = 0.2, \delta = 0.05$ and $t/P = 0.1$, where the dielectric filling is silicon ($n = 3.48$) and the grating is suspended in air. It is much thinner and has a much smaller dielectric filling factor compared to other high Q gratings like the HCG [23,31]. In Fig. 4(b), the $\omega - \beta$ dispersion plot [39] is calculated and it shows the 1st order "dark" and "bright" modes (blue dashed and solid lines, respectively) excited in the grating in the subwavelength regime, while β is the propagation constant in z for a given frequency ω. The 2nd order "dark" mode (orange dashed line) is not excited because it is "completely dark" due to the reflection symmetry in the grating [33]. For thin "diatomic" gratings, the "dark" mode gives rise to a single sharp resonance in the spectrum, free of off-resonance contributions. We note that its resonance wavelength is very close to P ($\lambda_{res} / P \approx 1.018$) and this makes the grating an optically thin ($n_{eff} t / \lambda_{res} \approx (\gamma(n-1)+1)t / \lambda_{res} \approx 0.15$) design. A zoom-in of the resonance is shown at the inset of Fig. 4(a). The slight Fano shape indicates a weak interaction between the "dark" and the "bright" modes [42]. Compared to the Q factor (~40) of the guided mode resonance of a regular but otherwise identical ($\delta = 0$) grating, Q in the "diatomic" grating is increased by more than 20,000 times (blue curve in Fig. 4(a)). This impressive Q is achieved with a subcell difference $\delta = 0.05$, 5% of the period length P. A more aggressive design of $\delta = 0.02$ will

push the Q up to 10^7 as shown in Fig. 4(d) and this is possible (for example, when $0.5\mu m < P < 1\mu m$) using the state of the art fabrication techniques. Similar performance is observed when the "diatomic" grating sits on a substrate. In the presence of substrates, P will shrink by a factor of $\sim 1/n_{substrate}$ for the device to remain subwavelength, and t will be slightly larger to compensate for the additional phase of reflection from the substrate. All other parameters of the optimized design stay mostly unchanged.
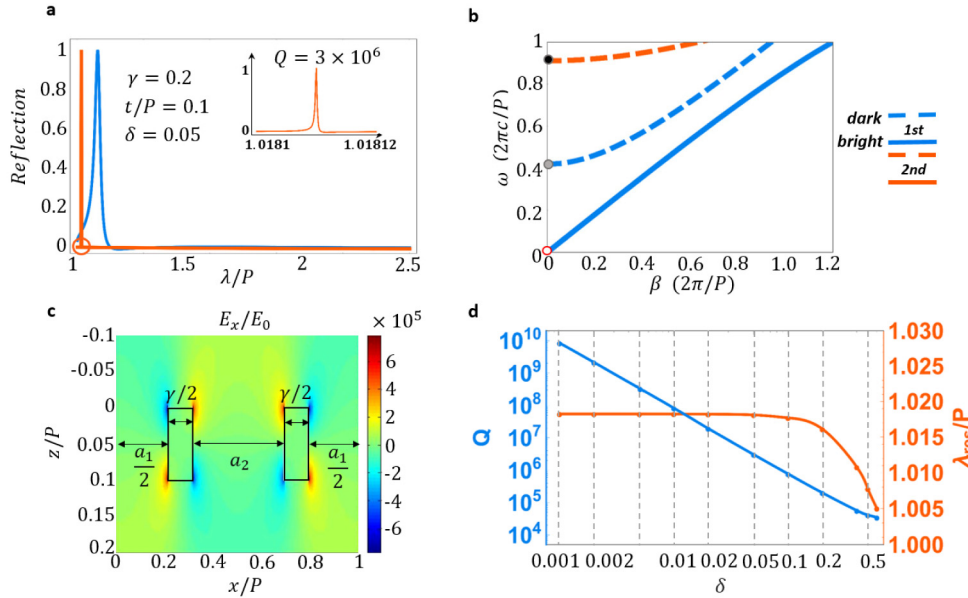

Fig. 4. The design of a typical single high Q resonance in a thin and small γ "diatomic" grating. (a) The single high Q resonance in the "diatomic" grating (red curve, zoom-in in the inset) and the moderate Q resonance in the corresponding regular grating (blue curve). (b) The mode dispersion ($\omega - \beta$) plot in the subwavelength regime showing both the 1st "bright" mode (blue solid line) and the 1st "dark" mode (blue dashed line) for the design. They are marked with red and gray dots respectively. The 2nd "dark" mode is completely dark due to the reflection symmetry of the grating and is marked by a dark dot. (c) The Electric field (E_x) enhancement inside the "diatomic" grating at resonance. The field enhancement is as high as 6×10^5. (d) Blue curve (log-log plot) depicts power law dependence of Q as a function of δ for the "dark" mode resonance. Orange curve shows the resonance wavelength barely changes with a large range of δ from 0.001 up to 0.1.

In the log-log plot of Fig. 4(d), Q diverges as $\delta \to 0$. When $\delta = 0$ exactly, the "dark" mode resonance disappears due to its complete darkness. The scaling law of Q on δ is consistent with Eq. (2). It is notable that the resonance wavelength λ_{res} remains flat for a broad range of δ up to $\delta = 0.1$, indicating that while $|r|$ of the "dark" mode varies dramatically, its round trip phase is not much affected by δ with changes by as large as 100 times. Therefore the parameter δ provides an effective control of Q in the design of "diatomic" gratings. From Eq. (2), one can obtain the approximate function for fabrication tolerance of Q in terms of δ as $d\delta/\delta \sim |dQ/Q|$, a linear relation. We can also infer from Fig. 4(d) that the fabrication tolerance for λ_{res} in terms of δ is extremely high up to $\delta = 0.1$. In Fig. 4(c), we see that the enhanced (up to 10^5 times) E_x field is largely concentrated in air gaps at resonance, consistent with the field profile for the 1st "dark" mode plotted in Fig.

1(d). This is very similar to plasmonic resonators designed for sensing [43], except that the parasitic photonic loss in metal is absent [44]. This very thin ($t/P \leq 0.1$) and very small filling factor ($\gamma \leq 0.2$) design makes the "diatomic" grating appealing for sensing applications that require both high Q resonance and a planar geometry for potential integration with 2D materials [21].

4. Application

One major advantage of the symmetry-broken "dark" modes in "diatomic" gratings is their robustness to strong external perturbation. This is expected in our previous discussion because of their structurally defined κ. As an important example, resonance wavelength (λ_{res}) of those dark modes can be tuned continuously in situ without degrading the Q, while the perturbation is provided by stretching the grating using a flexible substrate. A possible way to realize this idea is to embed silicon nano-pillars in the flexible PDMS substrate followed by the subsequent removal of PDMS to create a window of suspended silicon bars. The structure is supported by remaining PDMS at its periphery as illustrated in Fig. 5(b). By stretching PDMS using electro-mechanically applied stress (MEMS, for example), we can vary the period P in situ, while the widths of silicon bars remain unchanged. As a result, $\arg(r)$ (phase of the reflectivity) of the "dark" mode in the grating is continuously tuned [32] and λ_{res} is shifted. We study the tuning capability of the stretched "diatomic" grating by simulating its reflection spectrum using RCWA. The design parameters are $\gamma = 0.2, \delta = 0.05$ and $t/P = 0.1$. A tuning range ($\Delta\lambda/\lambda_0$) of 40% achieved by stretching the substrate up to 1.4 times ($1 + \Delta P/P_0$) is shown in Fig. 5(a) (blue solid line). The orange solid curve shows a sustained high Q cross the tuning range without deterioration. To compare with a representative regular grating (HCG) that also supports high Q resonances [23] ($\gamma = 0.7, t/P = 0.841$), the improvement of Q in the "diatomic" grating is up to 1000 times and its tuning range is ~10 times better. We see similar results for "diatomic" designs with larger δ, indicating that the improvement is quite universal. The reason for the rapid drop in Q in the HCG is because that the existence of their high Q modes depends sensitively on particular combinations of P and t [23]. This is overcome in the "diatomic" grating since: 1, the existence of 1st order dark mode in the subwavelength regime is guaranteed and 2, κ of the "dark" mode is structurally defined and it is minimally affected during stretch. The tuning capability of the "diatomic" grating approaches that of the ideal case (invariant λ_{res}/P) because $\lambda_{res} \sim P$ always holds in the design. This is desirable for applications that requires optimal tunability, like a tunable pixel in a display [45]. The "diatomic" grating is therefore an appealing candidate for planar resonators with tunable high Q resonances, whose practical design is still lacking to our best knowledge.
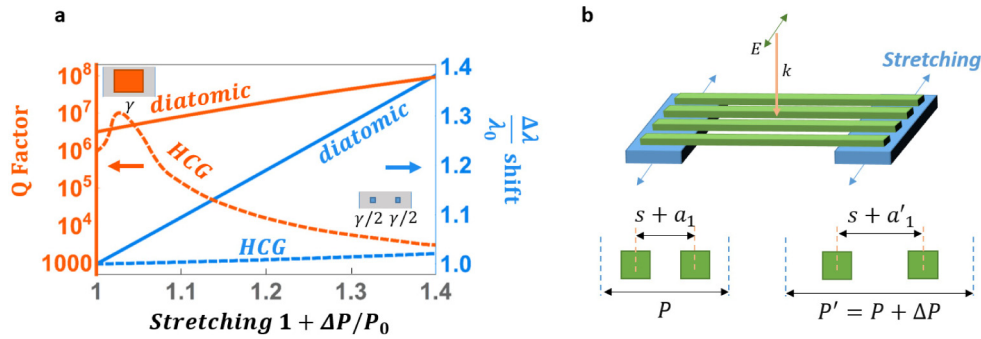
Fig. 5. In situ tuning of the high Q resonance in "diatomic" gratings. (a) Solid and dashed curves represent the simulation results of a typical "di atomic" and HCG grating respectively. Blue lines are the relative resonance shift ($\Delta\lambda/\lambda_0$) while orange lines are Q factors at the corresponding resonances. Inset shows the unit cell of HCG (orange) and "diatomic" (blue) gratings reflecting their design parameters for comparison used in the simulation. $P=1$ is assumed. The blocks represent silicon bars. (b) A schematic view of the structure that allows for in situ mechanical tuning of the grating period. Light is of TM polarization and normal incidence. It also gives an example of how the geometry of the grating changes after stretching from P to $P+\Delta P$, where s and a_1 are defined previously in the text.

5. Summary

We have theoretically studied a new class of 1D subwavelength gratings that supports tunable high Q resonances by breaking the symmetry between its unit cells. Optimization of the new structure, called the "diatomic", results in an ultra high Q resonance in a thinner grating with smaller filling factors compared to conventional gratings like HCGs. It offers unique advantages in terms of design flexibility and high Q sensing. Most importantly, we show that the resonance wavelength of the "diatomic" grating can be tuned in situ, exhibiting a close to ideal tuning range without compromising its Q. This work provides insight and design guidelines for this new class of planar resonators that are appealing to a wide range of applications including optical sensing, filtering and displays.

Acknowledgment